GENERAL INVERSE & ITERATION

IN TRAVEL TIME TOMOGRAPHY & EARTHQUAKE LOCATION

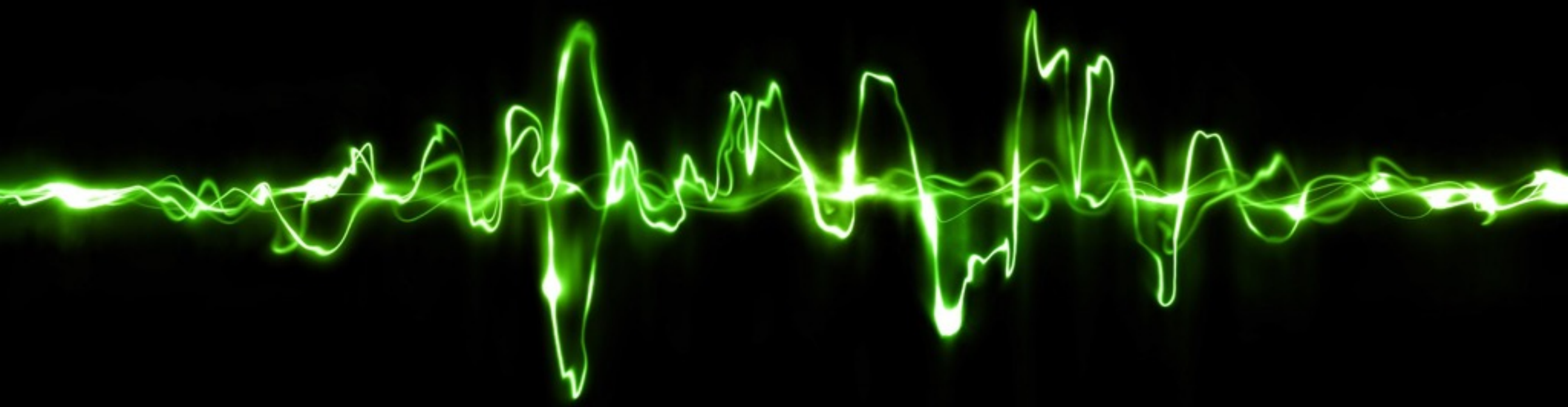

李智

PB13000383

SEISMOLOGY

I. Earthquake itself,

i.e. source, mechanism

II. Structure

i.e. wave propagation

Forward modeling

结构->观测 $\mathbb{F}(m) = d$

Inversion

观测->结构 $m = \mathbb{F}^{-1}(d)$

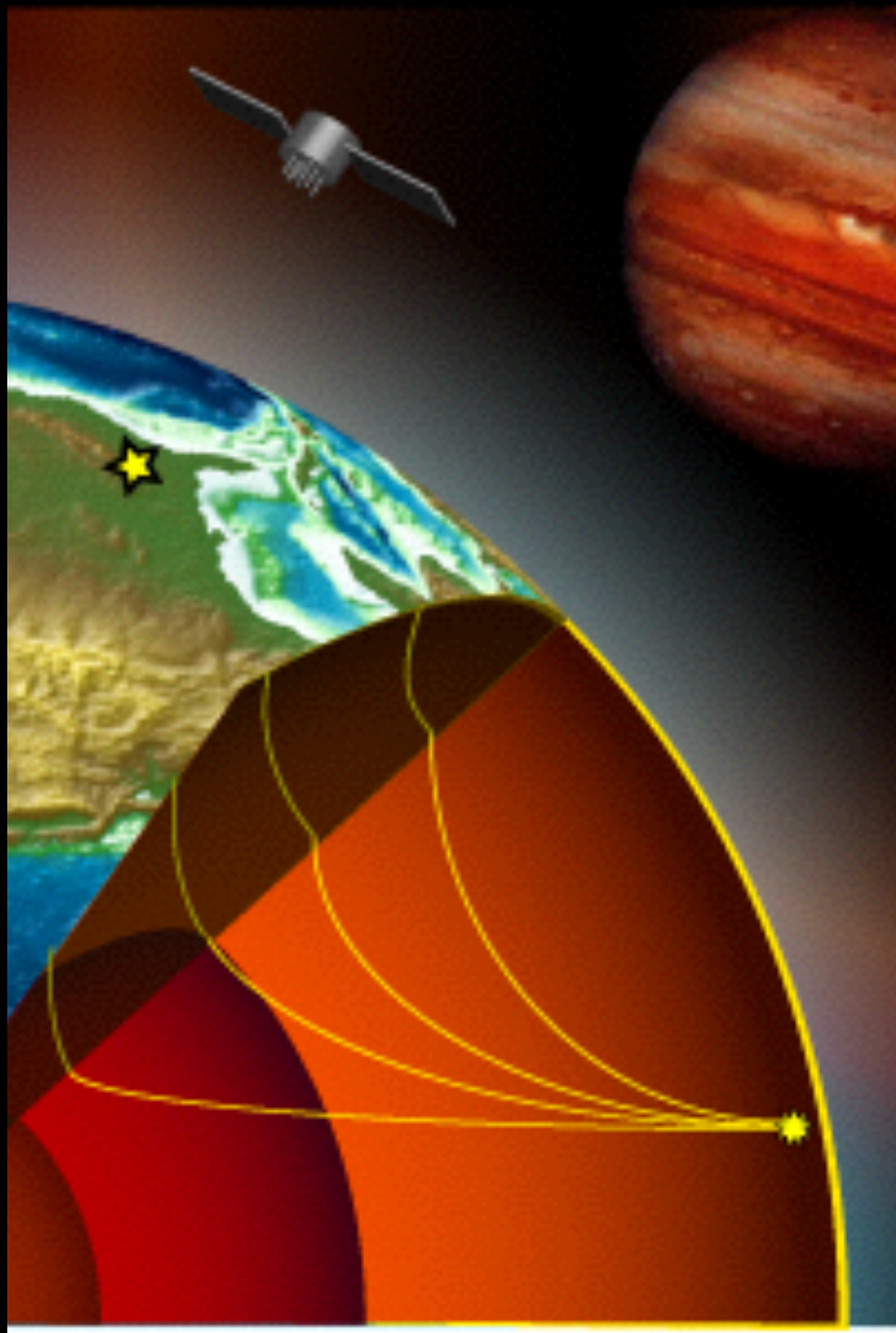

CONTENT

- Seismic Tomography (Travel time)
- Earthquake Location
- Related Research
  - —Tomographic inversion of Pn travel times in China

SEISMIC TOMOGRAPHY(TRAVEL TIME)

1. Travel time residual

$$t_{res} = t_{obs} - t_{pre}$$

t_{res} could come from:

a) Earth structure
b)Earthquake location error
c)Measurement errors

Seismic tomography:
$t_{res} \rightarrow$ 3D velocity perturbation, i.e $\delta v, \frac{\delta v}{v}$ (参考模型)

SEISMIC TOMOGRAPHY

2. Basic approach:

- Fermat Principle: the ray path between 2 points is such that the travel time along the path is stationary (minimum or maximum).

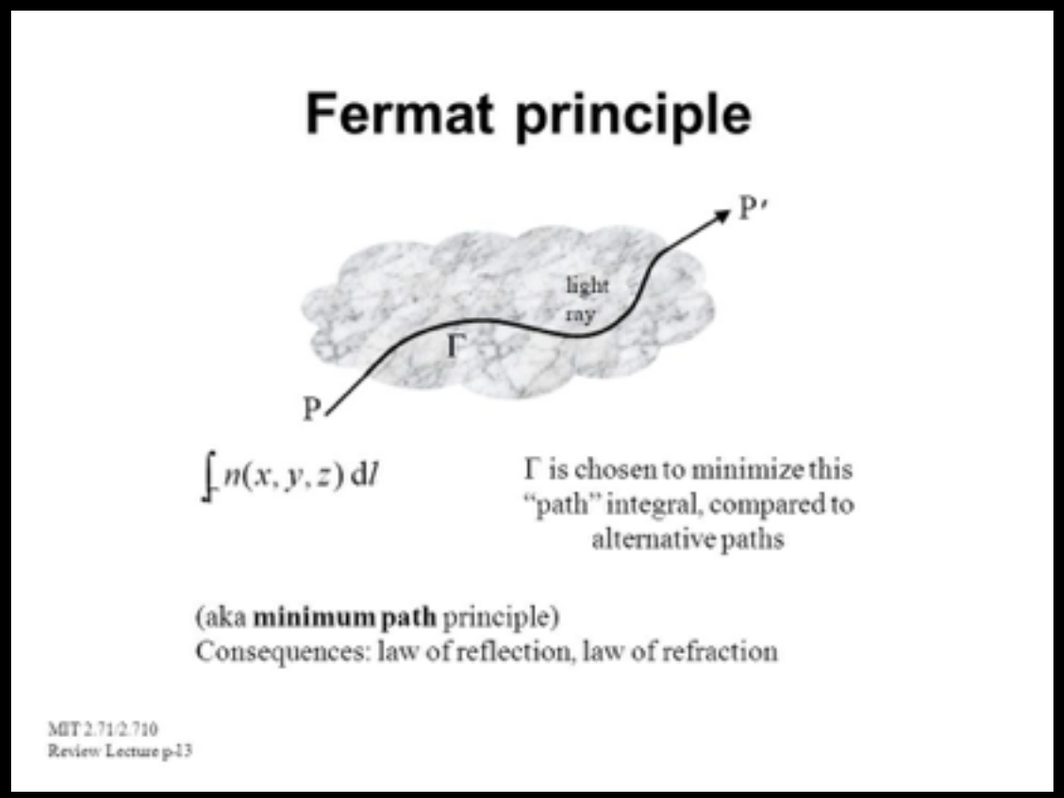

$$\delta t = \int_{L+\Delta l} \frac{ds}{v} - \int_{L} \frac{ds}{v} = 0$$

Thus, the travel time perturbation is:

$$\delta t = t - t_0 = \int_{L} \frac{ds}{v} - \int_{L_0} \frac{ds}{v_0}$$

(Fermat Principle)
$$\simeq \int_{L_0} \frac{ds}{v} - \int_{L_0} \frac{ds}{v_0}$$

SEISMIC TOMOGRAPHY

$$\delta t = t - t_0 = \int_L \frac{ds}{v} - \int_{L_0} \frac{ds}{v_0} \simeq \int_{L_0} \frac{ds}{v} - \int_{L_0} \frac{ds}{v_0}$$

$$= \int_{L_0} \delta(\frac{1}{v}) ds = -\int_{L_0} \frac{\delta v}{v^2} ds = -\int_{L_0} \frac{\delta v}{v} dt$$

$$= \int_{L_0} \delta u \, ds \quad \text{where} \quad u = \frac{1}{v} \text{ is slowness}$$

$$\Delta t_i = \sum_j l_{ij} \cdot \Delta u_j$$

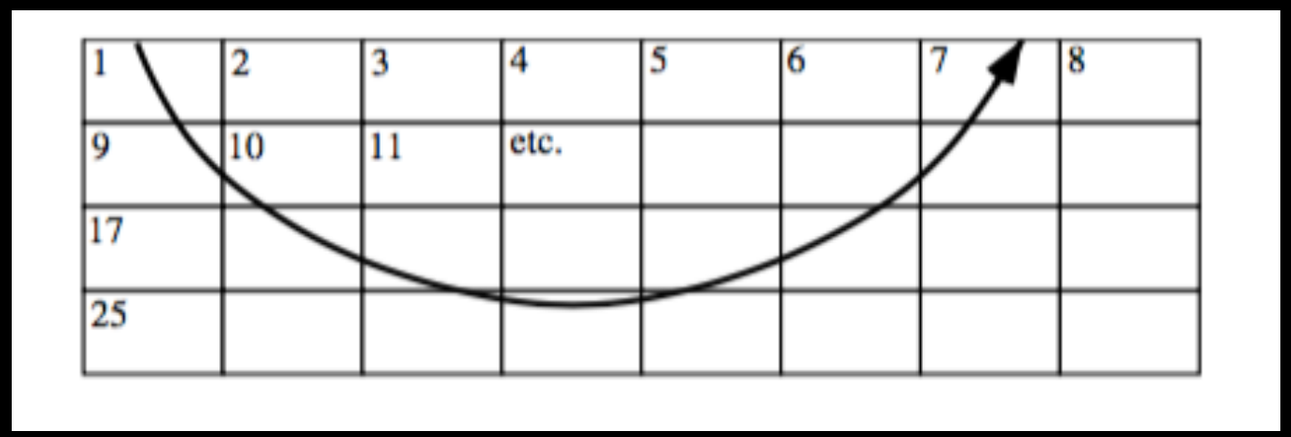

l_{ij} is the length of ray i in cell j <—sparse!

Δu_j is the slowness perturbation of in cell j <— what we want!

SEISMIC TOMOGRAPHY

Mathematically,
we have Matrix Form:

$$GM = d$$

A. DISCRETIZATION
B. LINEARIZATION

$G_{ij} = l_{ij}$ G — data kernel

$m_j = \Delta u_j$ m — model parameter

$d_i = \Delta t_i$ d — data

SEISMIC TOMOGRAPHY

- The problem is generally overdetermined: $G_{mn}, m > n$

Solution 1: $G^{\mathrm{T}}GM = G^{\mathrm{T}}d$

$$M = \underline{(G^{\mathrm{T}}G)^{-1}}Gd$$

This minimize $\sum (d_i - G_{ij}M_j)^2$

Solution 2: $f(M_j) = \sum (d_i - G_{ij}M_j)^2 + \underline{\lambda \, \mathrm{l}\, m \, \mathrm{l}^2}$

damping

$$\frac{\partial f}{\partial M} = 0$$

EARTHQUAKE LOCATION

1. Preliminary location

- Distance can be estimated from S-P time.

- For Possion solid:

$$x = \frac{t_s - t_p}{\sqrt{3}-1} v_p \sim (t_s - t_p) \times 8 km/s$$

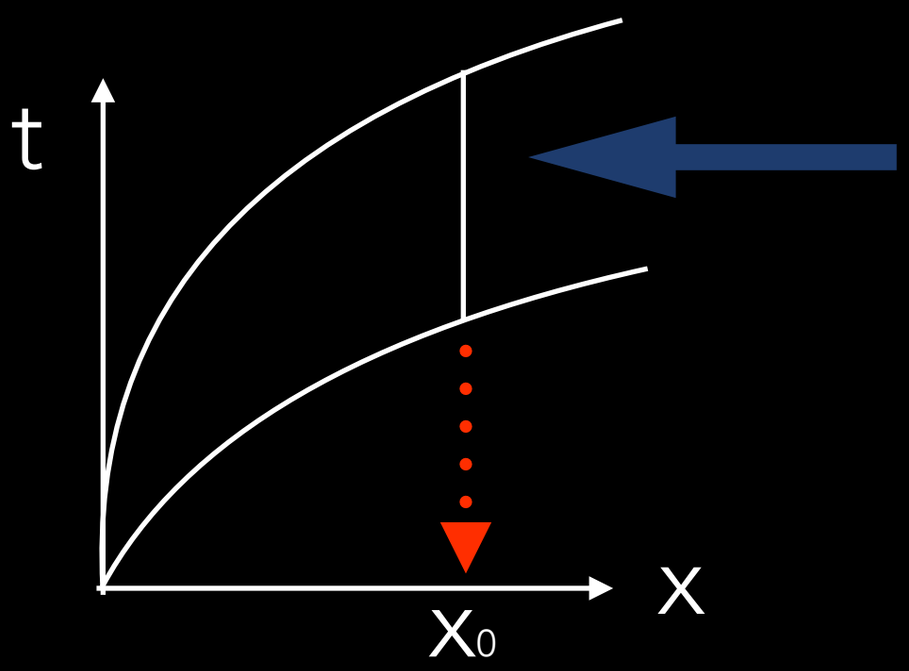

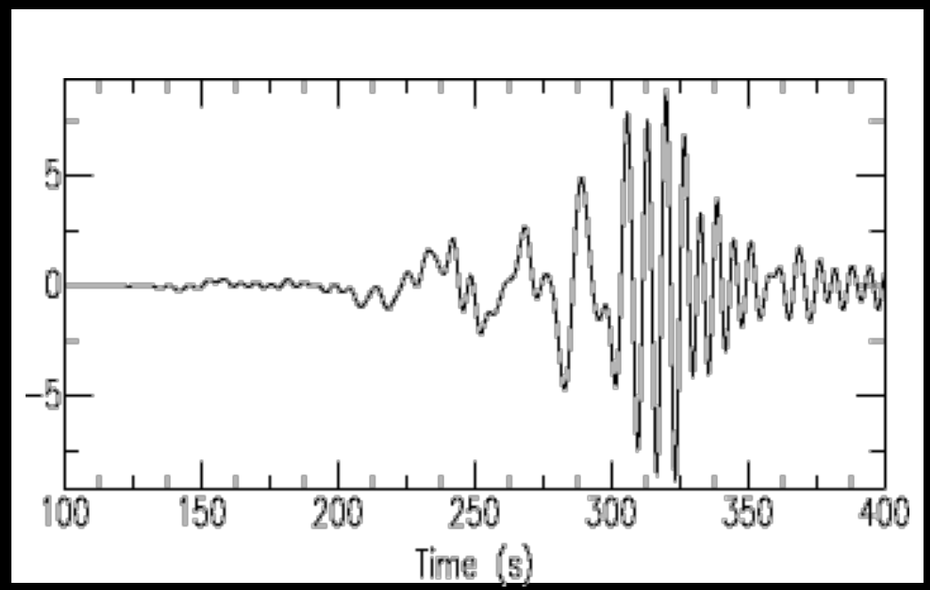

EARTHQUAKE LOCATION

- Theoretically, with 3 or more stations we can find an epicenter

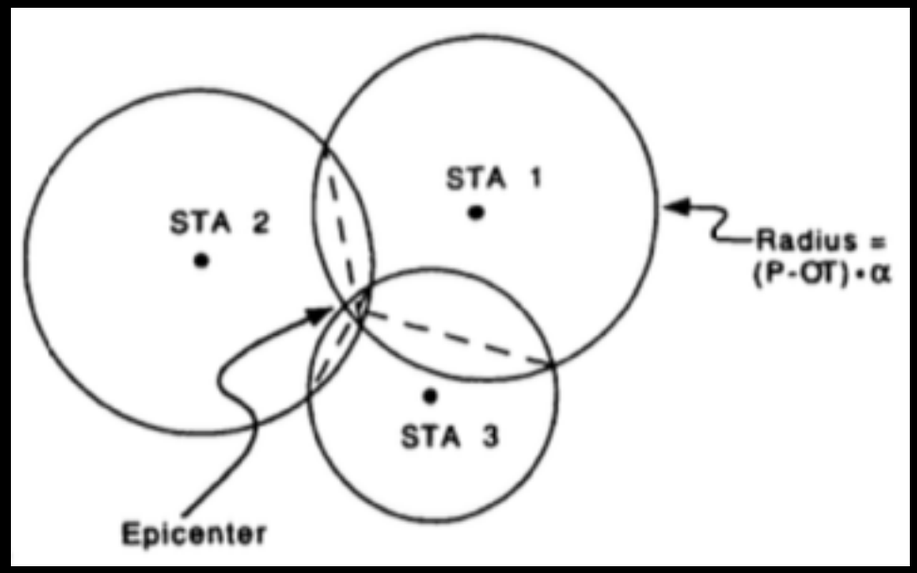

- Focal depth can be estimate via pP-P depth phase

EARTHQUAKE LOCATION

2. Iterative location methods

- Arrival time at station n
- =travel time + origin time

$$T(\vec{x},\vec{x_i})+t$$

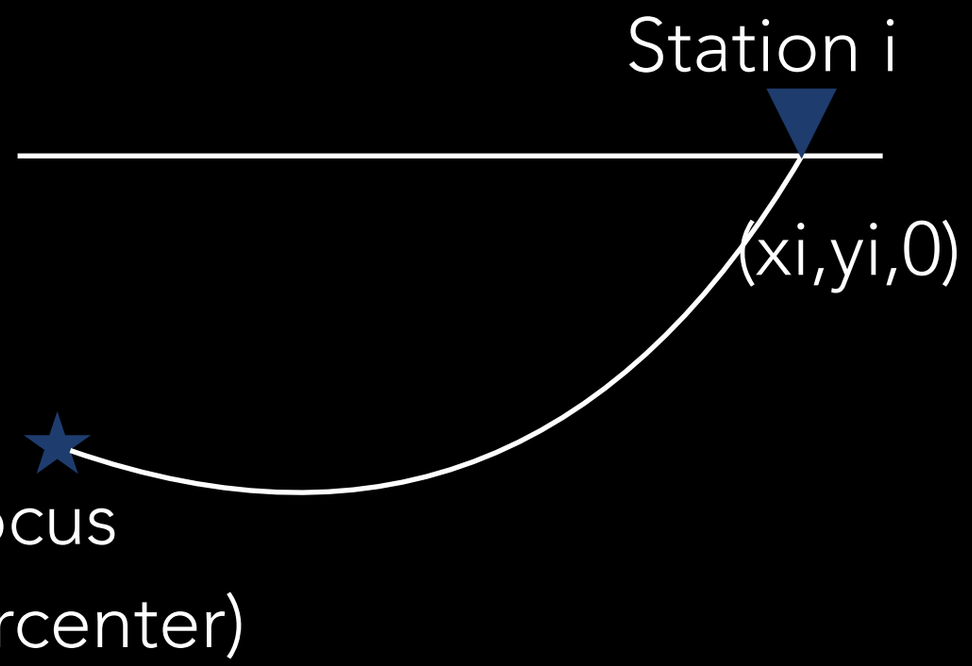

EARTHQUAKE LOCATION

we can cast the problem as an inverse problem

$$\vec{d} = A(\vec{m})$$

where d is data (observations), m is model parameters function A is known once M is known.

we solve by iteration. Regard m as a perturbation to a starting model. $\vec{m} = \vec{m_0} + \Delta\vec{m}$

we seek $\Delta\vec{m}$, by solving linearized equation:

$$d_i = d_i^0 + \varepsilon \left.\frac{\partial d_i}{\partial m_j}\right|_{m_0} \cdot \Delta m_j$$

EARTHQUAKE LOCATION

- Matrix Form:

$$G\Delta M = \Delta d$$ (Over-determined)

$$G_{ij} = \frac{\partial d_i}{\partial m_j}\Big|\vec{m}_0$$ (Evaluated for m_0)

$$\Delta d_i = d_i - d_i^0$$

- Generalized Inverse:

$$\Delta m = (G^{\mathrm{T}}G)^{-1}G\Delta d$$

$$|G\Delta M - d|^2 = \sum_i (\sum_j G_{ij}\Delta m_j - \Delta d_i)^2$$

Update $\vec{m} = \vec{m}_0 + \Delta\vec{m}$ and iterate until converage

EXAMPLE:

3. Earthquake location for homogenous medium

Source $\vec{x} = (x, y, z)$

Station $\vec{x}_i = (x_i, y_i, 0)$

Arrival time: $d_i = T(x, x_i) + t = \frac{1}{v}[(x - x_i)^2 + (y - y_i)^2 + z^2]^{1/2} + t$

$$G_{i1} = \frac{\partial d_i}{\partial m_1} = \frac{\partial d_i}{\partial x} = \frac{x - x_i}{v}[(x - x_i)^2 + (y - y_i)^2 + z^2]^{-1/2}$$

$$G_{i2} = \frac{\partial d_i}{\partial m_2} = \frac{\partial d_i}{\partial y} = \frac{y - y_i}{v}[(x - x_i)^2 + (y - y_i)^2 + z^2]^{-1/2}$$

$$G_{i3} = \frac{\partial d_i}{\partial m_3} = \frac{\partial d_i}{\partial z} = \frac{z}{v}[(x - x_i)^2 + (y - y_i)^2 + z^2]^{-1/2}$$

$$G_{i4} = \frac{\partial d_i}{\partial m_4} = \frac{\partial d_i}{\partial t} = 1$$

EARTHQUAKE LOCATION

- The iteration to find locations

Given di, initial velocity model

—> Assume starting model $\vec{m}_0 = (x, y, z, t)$

—> Calculate

$d_i = T(x, x_i) + t$ and $G_{ij}, j = 1,...4$ for each station i

—> $\Delta m = (G^{\mathrm{T}} G)^{-1} G(d_i - d_i^0)$ (Generalized Inverse)

—> $\vec{m} = \vec{m}_0 + \Delta\vec{m}$

EARTHQUAKE LOCATION

4. Earthquake location in realistic earth

- location parameters in spherical coordinates:

$\vec{m} = (t, \theta, \phi, h)$, where $\theta = 90^\circ - \text{lat}$ is colatitude from 0~180

Regard m as a perturbation to a starting model m_0

$$\vec{m} = \vec{m}_0 + \Delta\vec{m}$$

First order approximation of arrival time is:

$$d_i^p(\vec{m}) \simeq d_i^p(\vec{m}_0) + \Sigma \frac{\partial d_i}{\partial m_j} \Delta m_j$$

In matrix form: $\frac{\partial d_i}{\partial m_j} \Delta m_j = d_i^{obs} - d_i^p(\vec{m}_0)$

$d_i^p(\vec{m}_0)$ predicated arrival time at its station for m_0

$\frac{\partial d_i}{\partial m_j}$ is evaluated for model m_0

EARTHQUAKE LOCATION

Similarly, $\Delta\vec{m}$ can be found using generalized inverse, update $\vec{m} = \vec{m}_0 + \Delta\vec{m}$ and iterate the above process until $\Delta\vec{m}$ is small enough (location converge)

- The partial derivatives (in spherical geometry)

$$\frac{\partial d^P}{\partial t} = 1$$

(See David Gubbis P119)

$$\frac{\partial d^P}{\partial h} = -\frac{1}{r}\left(\frac{r^2}{v} - p^2\right)^{1/2}$$

r is radius

$$\frac{\partial d^P}{\partial \theta} = p\cos z$$

p is ray parameter

$$\frac{\partial d^P}{\partial \phi} = -p\sin z\sin\theta$$

z is azimuth

p can be found retracing or from travel time table $p = \frac{dT}{d\Delta}$

Tomographic inversion of Pn travel times in China

The Pn travel time is the sum of the travel time in the crust from the source to the Moho and from the Moho to the receiver, and the travel time of the head wave traveling at the top of the upper mantle, (Right Figure)

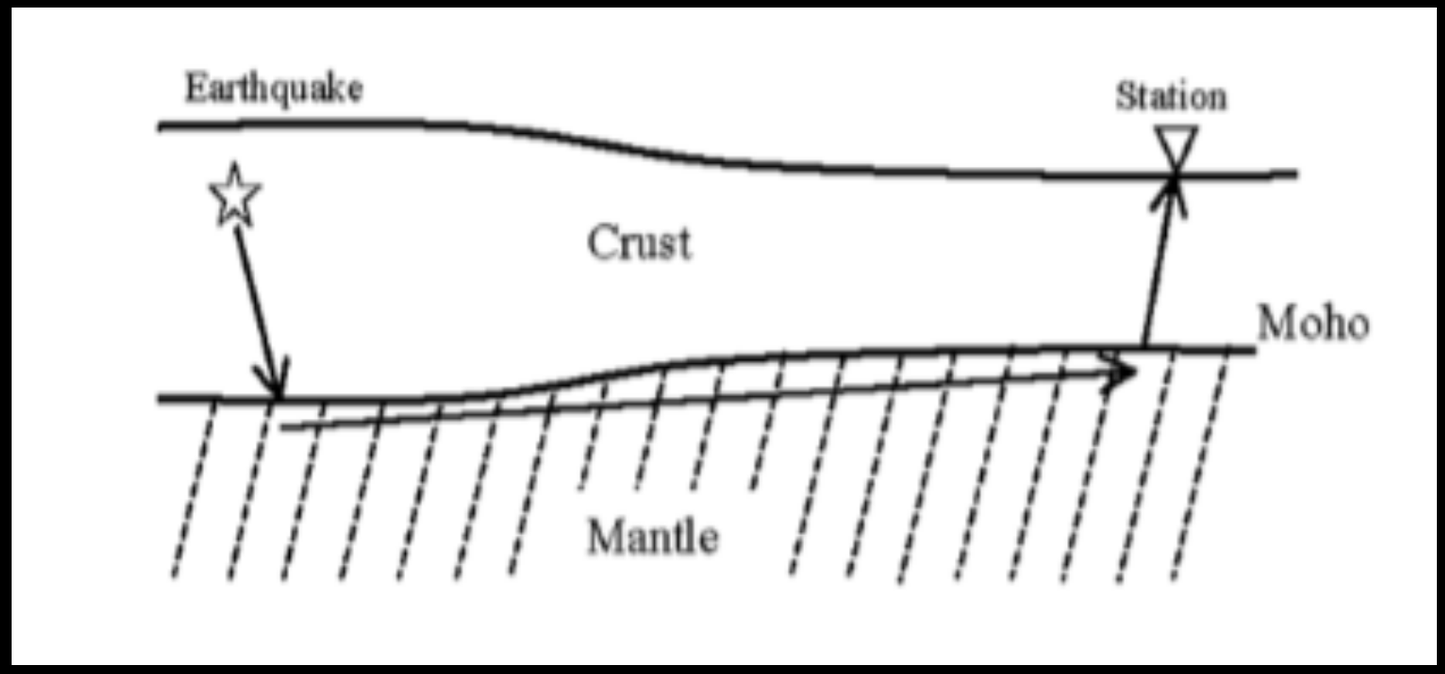

Schematic diagram of Pn wave propagation. The P wave is critically refracted at the Moho boundary. The ray path has three segments, associated with the source, the receiver, and the mantle. Our tomographic inversion solves for the static delay times in the crust associated with the earthquake and the station and the lateral velocity variation and the velocity anisotropy at the top the mantle encountered by the mantle segment of the ray path.

See van der Hilst et al. [1997], Grand et al. [1997] and Hearn [1996]

2. Inversion Method

[11] We follow the basic inversion scheme of *Pn* waves by *Hearn* [1996]. The *Pn* travel time is the sum of the travel time in the crust from the source to the Moho and from the Moho to the receiver, and the travel time of the head wave traveling at the top of the upper mantle (Figure 2). We divide the study area into two-dimensional (2-D) cells of 0.5° by 0.5° along the longitudes and latitudes. Thus the *Pn* travel time residual (the observed travel time minus the predicted travel time for a reference model) can be written

$$\Delta t_{ij} = \Delta t_i^{eq} + \Delta t_j^{st} + \sum_{k=1}^{N} d_{ijk}\Delta s_k + \sum_{k=1}^{N} d_{ijk}\cos(2\phi_{ijk})a_k + \sum_{k=1}^{N} d_{ijk}\sin(2\phi_{ijk})b_k, \quad (1)$$

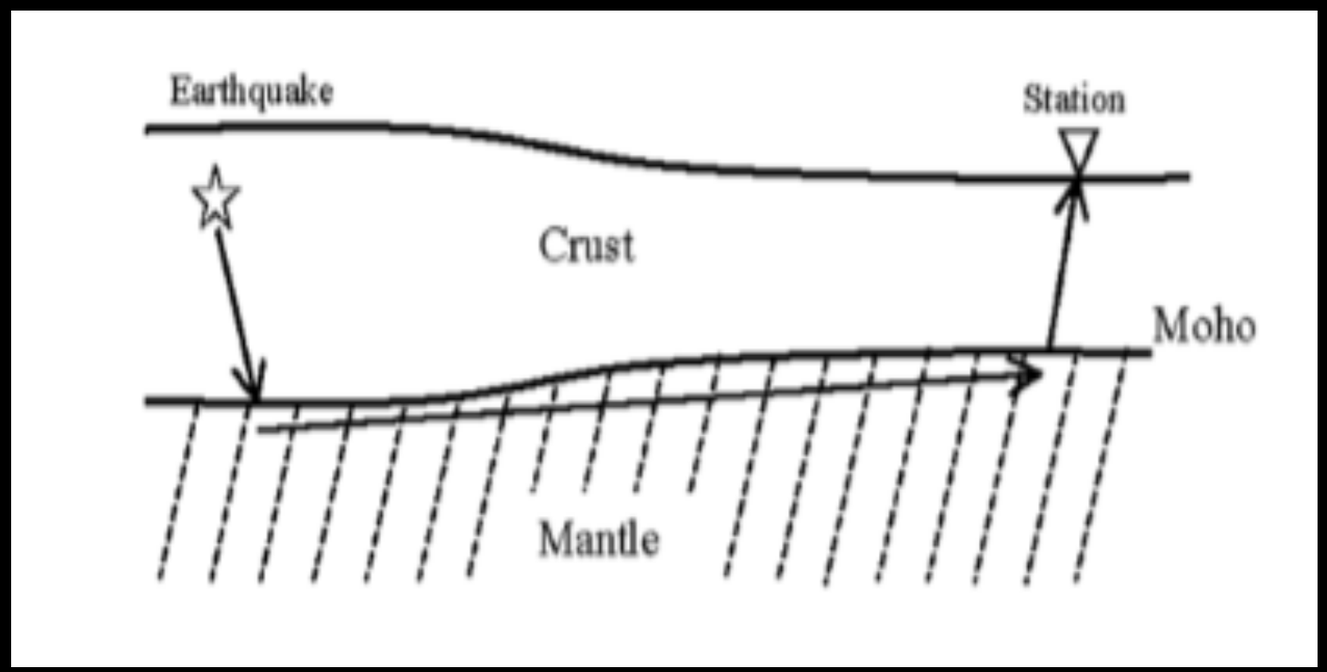

$$d = Gm$$

1965]. Note that we use the azimuth of the ray at each cell (ϕ_{ijk}) instead of the same azimuth (or back azimuth) of the ray for all cells along the ray [*Hearn*, 1996], because the azimuth (back azimuth) may change substantially along the ray. The magnitude of anisotropy at cell k is given by $(a_k^2 + b_k^2)^{1/2}$ and the direction of fastest wave propagation is given by arctan $(b_k/a_k)/2$ from the north.

[12] The linear system of equations (1) can be written in matrix form:

$$\mathbf{d} = \mathbf{Gm}, \quad (2)$$

where **d** is the data vector whose elements are the observed residuals of rays Δt_{ij}, and the number of the elements is equal to the number of rays; the solution vector **m** comprises all the model parameters we want to solve: earthquake and station delays (Δt_i^{eq} and Δt_j^{st}), and *Pn* slowness perturbation Δs_k and anisotropy parameters a_k and b_k in every cell; the matrix **G** is called the data kernel, which relates the data (observed residuals) and the

$$\Delta t_{ij} = \Delta t_i^{eq} + \Delta t_j^{st} + \sum_{k=1}^{N} d_{ijk}\Delta s_k + \sum_{k=1}^{N} d_{ijk}\cos(2\phi_{ijk})a_k + \sum_{k=1}^{N} d_{ijk}\sin(2\phi_{ijk})b_k$$

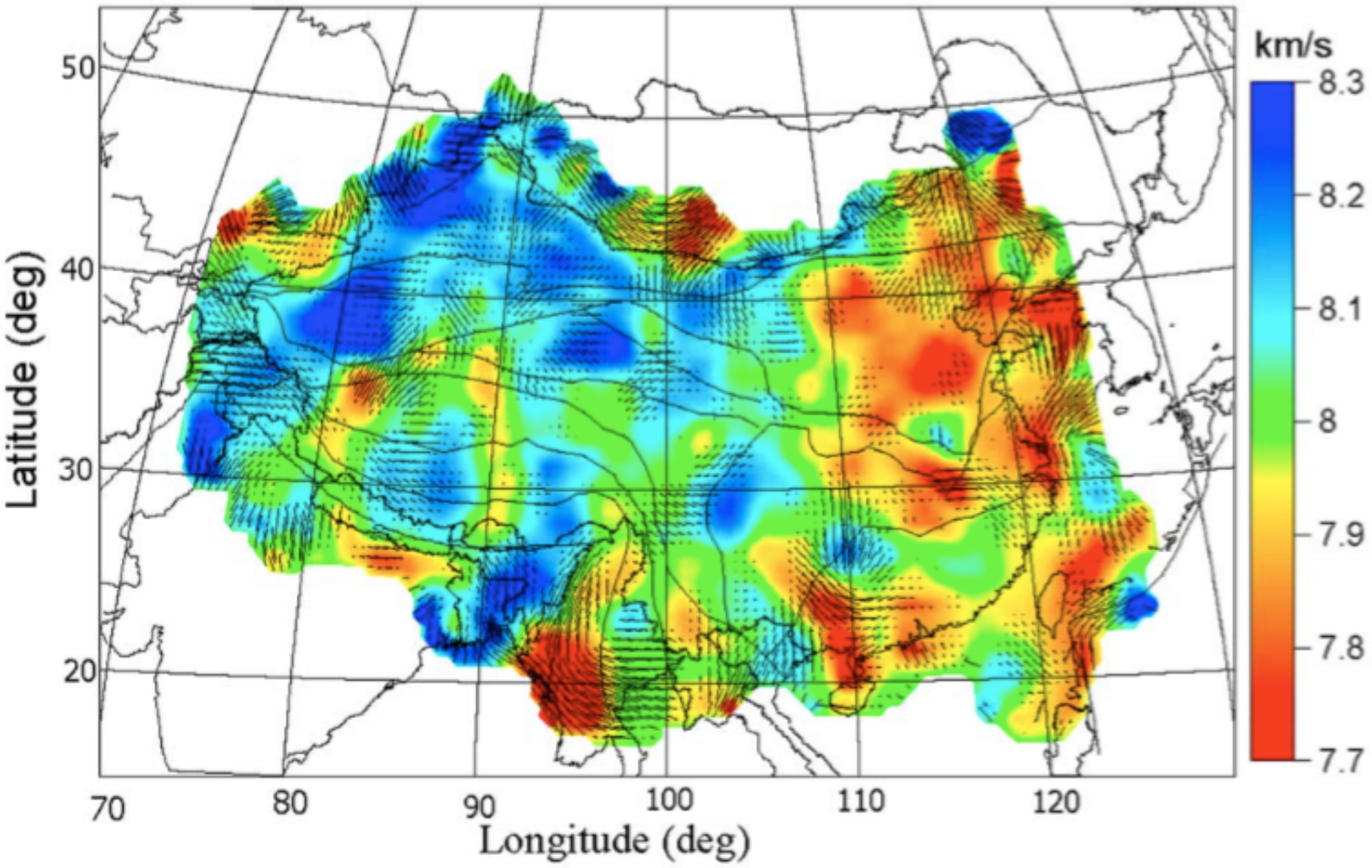

Figure 7. Inversion results for *Pn* velocity (color) and anisotropy (bars). Red and blue indicate saturated for low velocity at 7.7 km/s and for high velocity at 8.3 km/s, respectively. The bar indicates the fast *Pn* direction, and the length is proportional to the anisotropy amplitude, saturated at 4%. Only anisotropies larger than 1% are plotted. Also plotted are major block boundaries (Figure 1) as well as country borders and coastlines.

$$\Delta t_{ij} = \Delta t_i^{eq} + \Delta t_j^{st} + \sum_{k=1}^{N} d_{ijk}\Delta s_k +$$

$$\sum_{k=1}^{N} d_{ijk}\cos(2\phi_{ijk})a_k + \sum_{k=1}^{N} d_{ijk}\sin(2\phi_{ijk})b_k$$

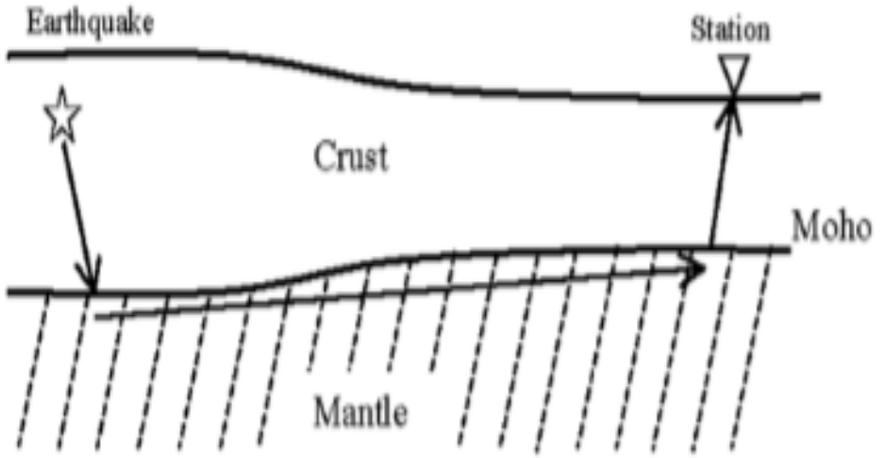

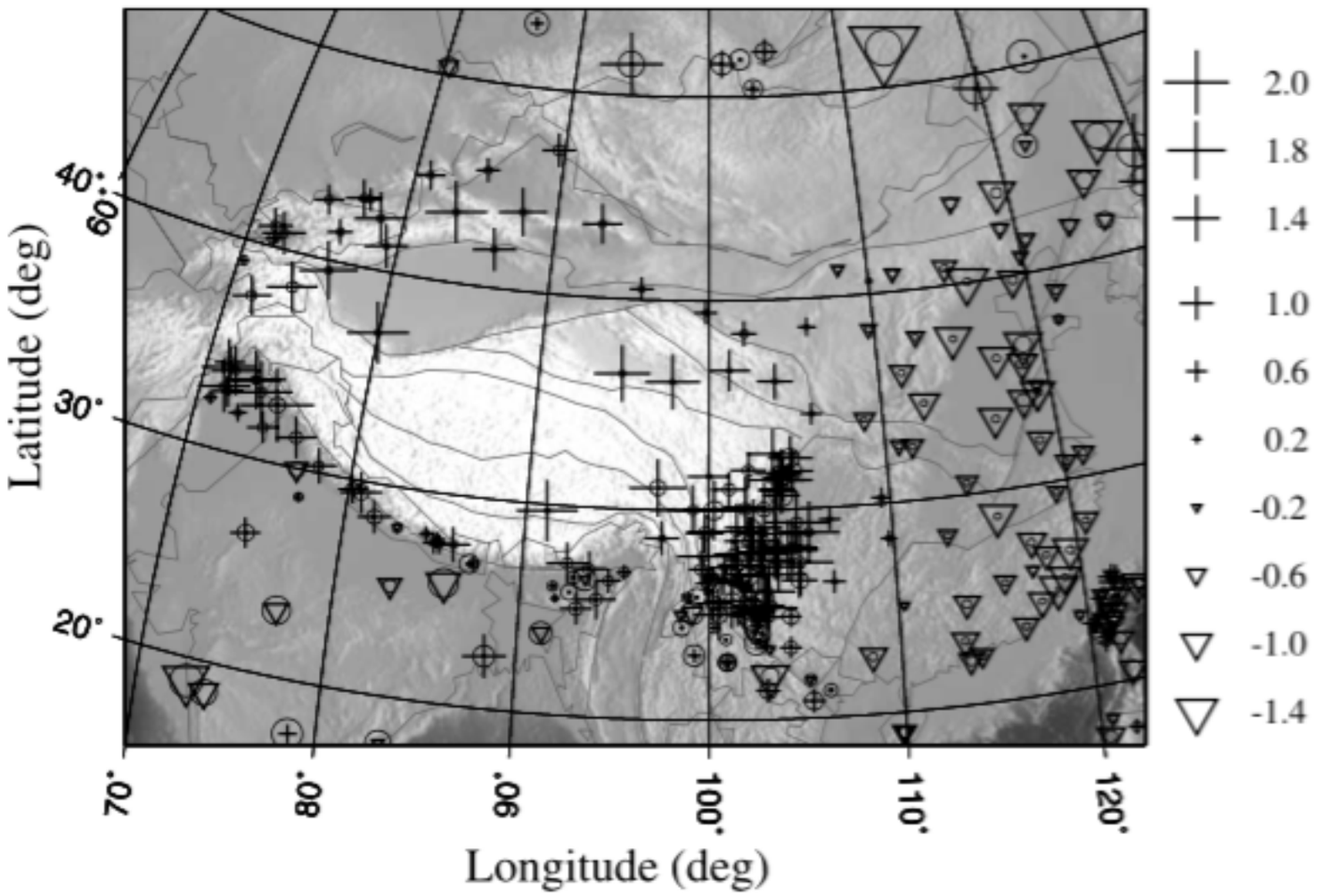

Figure 8. Station delays obtained in this study. Negative delays (triangles) is indicative of a thinner crust (thinner than the average 43.8 km of the reference model); positive delays (crosses) is indicative of a thicker than average crust. Circle indicates the standard error of the corresponding station delay.

$$\| Gm - d \|^2 + \lambda^2 \| Lx \|^2$$

Smoothness
Singularity
Damping

[15] Because of uneven distribution of ray paths and data errors, the linear system (2) or (3) is generally highly ill-conditioned, which may result in singularities with extremely high or low values in local areas and make the inversion unstable. A common approach in dealing with the problem is to impose additional constraints to regularize the solutions [*Van Der Sluis and Van Der Vorst*, 1987]. Here we impose the smoothness constraints as described by *Lees and Crosson* [1989]. Because our slowness solution is a discrete version of the continuously varying field, it is desirable to have some constraints for our solutions to have a certain measure of roughness. Smoothed solutions also allow us to concentrate on more coherent large-wavelength structures and ignore local small-scale variations in interpreting inversion results.

[16] The smoothness constraints are imposed by minimizing the Laplacian (second derivative) of the solutions $\mathbf{m}'$ (instead of $\mathbf{m}$). Thus our LSQR solutions minimize the following damped least squares functional: $\|\mathbf{G}'\mathbf{m}' - \mathbf{d}\|^2 + \lambda^2\|Lx\|^2$. Here $\|\mathbf{v}\|$ denotes the Euclidean (L_2) norm with $\|\mathbf{v}\|_2 = (\mathbf{v}^T\mathbf{v})^{1/2}$, and the Laplacian operator L is applied to the component $\boldsymbol{x}$ of $\mathbf{m}'$ that corresponds to slowness or either anisotropic coefficient. The parameter λ controls the level of smoothing, which trades off with the misft (error reduction) $\|\mathbf{G}'\mathbf{m}' - \mathbf{d}\|$. As λ increases, the inversion image becomes smoother and the misfit increases. We choose $\lambda = 0.3$ in this study.

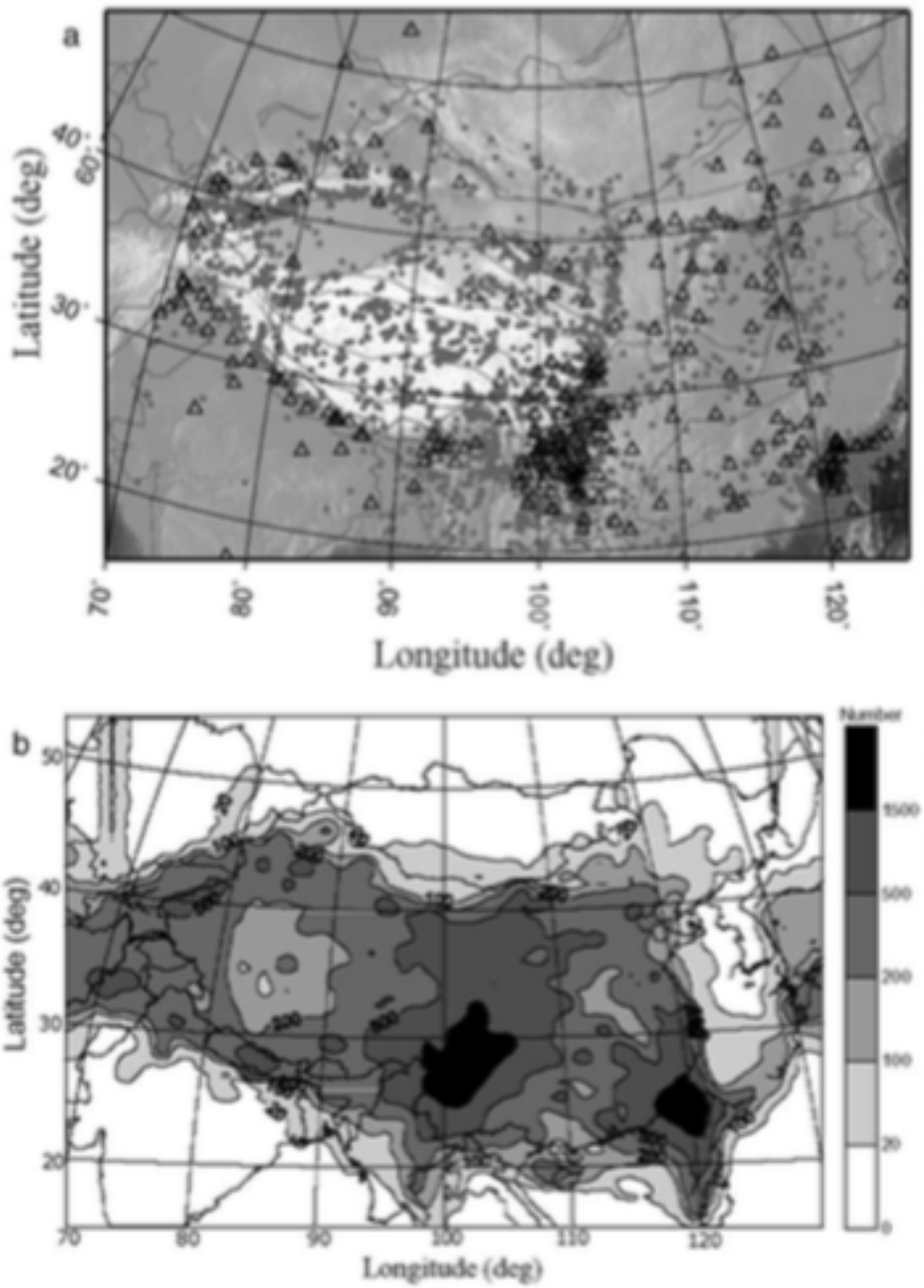

Figure 3. (a) Distribution of earthquakes (dots) and stations (triangles) and (b) the ray coverage used in this study. Plotted is the number of rays in each cell.

Ray Distribution

Pn theoretical travel time

Analytical solution

Ray shooting
Snell's Law

REFERENCE

Liang, C., X. Song, and J. Huang (2004), Tomographic inversion of Pn travel times in China, J. Geophys. Res., 109, B11304, doi:10.1029/2003JB002789.

Lay, T. and Wallace, T. C. (1995). *Modern Global Seismology*, San Diego: Academic Press.

Shearer, P. (1991). *Introduction to seismology*, Cambridge University Press

Stephane Mallet, (2009). *A Wavelet Tour of Signal Processing The Sparse Way,*

Manners, U. J., and Masters, G. (2008). Analysis of core-mantle boundary structure using S and P diffracted waves, *Geophys. J. Int.*

Shearer, P. M. and Chapman, C. H. (1988). Ray tracing in anisotropic media with a linear gradient, Geophys. J. Int., **94**, 575–80.

Shearer, P. (1991). Imaging global body wave phases by stacking long-period seismograms. / . *Geophys. Res.* 96, 20,353-20,364

Aki, K., and P. G. Richards (2002), Quantitative Seismology, 2nd ed., Univ. Sci. Books, Sausalito, Calif.

van der Hilst, R. D., S. Widiyantoro, and E. R. Engdahl (1997), Evidence for deep mantle circulation from global tomography, Nature, 386, 578– 584.

Hearn, T. M. (1996), Anisotropy Pn tomography in the west United States, J. Geophys. Res., 101, 8403–8414.

Grand, S. P., R. D. van der Hilst, and S. Widiyantoro (1997), Global seismic tomography: A snapshot of convection in the Earth, GSA Today, 7(4), 1–7.

THANK YOU!